BNL-101822-2014-TECH

AD/RHIC/RD/40;BNL-101822-2013-IR

Fracture Toughness Requirements for RHIC Cryogenic Design

S. Kane

May 1992

Collider Accelerator Department

Brookhaven National Laboratory

U.S. Department of Energy

USDOE Office of Science (SC)

DISCLAIMER

AD/RHIC/RD–40

RHIC PROJECT

Brookhaven National Laboratory

Fracture Toughness Requirements for RHIC Cryogenic Design

Steve Kane

May 1992

FRACTURE TOUGHNESS REQUIREMENTS FOR RHIC CRYOGENIC DESIGN

by Steve Kane

ABSTRACT

This paper provides a brief overview of fracture toughness and summarizes the results of research conducted in the past decade on cryogenic fracture toughness of wrought and weld austenitic stainless steel materials. This research has found that various composition elements have a significant effect upon material fracture toughness at 4K. Nitrogen is a strengthener and has been found to increase fracture toughness. Oxygen manifests itself in weld materials as inclusions and has a severe detrimental effect upon fracture toughness. This one factor largely accounts for the difference between wrought and weld material. This is found to be dependent upon the weld process, with TIG clearly excelling as the conventional process most consistently producing welds with low oxygen (inclusion) content.

Weld materials enhanced with manganese and higher nickel contents than standard compositions have demonstrated improved fracture toughness. Ferrite, both measured and calculated, and carbon content has significant deleterious effects upon austenitic stainless steel weld fracture toughness. Again, TIG welding demonstrates superior fracture toughness with commonly occurring ferrite content, while other processes require much lower ferrite numbers for similar fracture toughness. A relationship between yield strength and fracture toughness stress intensity factor (K_{IC}) shows that Type 316L weld metal can meet the needs of RHIC, but quality controls are required to meet the necessary fracture toughness with a 95% confidence level. Magnetic field effects are found to be inconsequential to fracture toughness for austenitic stainless steels.

Discussions with the National Institute of Standards and Technology indicate Type 316L is the weld material of choice for cryogenic applications and has superior fracture toughness well worth the minor price differential. Fracture mechanics analysis also shows Type 316L weld metal will meet RHIC requirements with proper quality controls. However, all research is based upon pure austenitic stainless steel welds and does not address welds contaminated by welding to ordinary carbon steel. A backup strip of austenitic stainless steel, and some quality controls, are necessary to meet fracture toughness requirements for the RHIC dipole design.

WHAT IS FRACTURE TOUGHNESS?

Fracture toughness is the term applied to a material mechanical property. This property is the material's resistance to catastrophic fracture in the presence of a defect. Defects are always present in any manufactured article. They may be occur as a result of the manufacturing process (dents, gouges, weld under-cut) or may be embedded within the material (cold lap, weld inclusion). Generally, fracture toughness decreases as a function of material strength and temperature. Steels are usually strengthened with carbon. Carbon tends to form martensite which has superior strength but poor ductility. Thus fracture toughness is a measure of ductility, or a material's ability to deform in a ductile manner without fracture. The cause for deformation may be from several sources. Generally, materials deform when the stress the material is subjected to stresses beyond its elastic limit. Materials fail or fracture when the stresses exceed the ultimate stress or ultimate strength. Materials with very high yield strengths usually have ultimate strengths very near the yield strength, hence very little deformation is associated with failure of 'high strength' materials. They appear to be 'brittle' and fail by fracture. Stresses in a material can be magnified by stress concentrators such as notches, cracks, or voids (defects). This magnification will cause the stresses near the defect to exceed the ultimate stress even though the adjacent material is subjected to very low stresses. If the material is ductile or has good fracture toughness, the crack or notch tip will deform and blunt, thereby reducing the stress concentration and the potential for fracture. However, if the material has poor ductility, hence poor fracture toughness, the crack or notch tip will not blunt and will propagate by fracture. Therefore the stress concentration is not reduced and the defect propagates uncontrollably to failure.

Martensitic transformation is generally a temperature and stress related phenomena. As temperature decreases or stress increases, martensite transformation increases. The temperature which triggers this transformation in ordinary steels is quite high, approximately -40 to -20^{O}F. Charpy V-Notch impact testing was developed to obtain a *relative* measure of a material's fracture toughness. It was quick and cheap, hence its adoption by the manufacturing community. Material development and research in the past 30 years has resulted in identification of other properties to better describe fracture toughness. Lateral expansion quantifies the deformation associated with impact testing and is preferred for low yield strength materials like austenitic stainless steels. Critical stress intensity factor, K_c K_{Ic}, was also identified for materials for *slow loading and linear elastic material behavior*. It is a measure of the material's ability to carry load or deform plastically in the presence of a stress concentrator (notch). Its relationship is best described by:

$$K_{Ic} \text{ or } K_c = C\sigma\sqrt{a}$$

where C is a function of the crack geometry, σ is stress and a is defect size. It is a direct function of material stress and defect size and configuration.

FACTORS AFFECTING CRYOGENIC STRENGTH

Austenitic weld material strength has been found to behave similar to wrought plate of the same composition. Below room temperature, strength increases as temperature is lowered. Some of the factors affecting cryogenic strength in wrought materials also affect weld materials.

MARTENSITIC TRANSFORMATION

Many austenitic stainless steels are metastable, tending to transform from a face-centered-cubic (FCC) structure to a more stable body-centered-tetragonal (BCT) martensite at low temperatures. Low temperature, mechanical stress, and the presence of a magnetic field will increase the driving force for transformation. Mechanical deformation may also facilitate transformation by promoting the nucleation of the martensite phase. The martensite is more brittle than FCC austenite. The reason for the brittleness is that when the body-centered-cubic (BCC) structure of ferrite is deformed there is a tendency for microcracks to be formed in the crystal. The intense stress concentration at the tip of such a crack causes it to extend, thereby producing rapid fracture. Testing has also showed that martensite will be transformed from metastable austenite phase not only by cyclic stressing but also by *static loading*[1]. Increasing amounts of transformed martensite generally act to increase tensile and yield strengths but decrease toughness at given temperatures.

NITROGEN

Austenitic stainless steels strengthened with nitrogen are becoming more common in industrial cryogenic applications. The nitrogen bearing austenitic steels which are commercially available have an austenitic microstructure which is highly stable. Unstable austenitic steels have the potential for transforming to hard martensite under deformation, particularly if interstitial nitrogen content is high. Some of the commercially available austenitic stainless steel, such as 304, have an unstable microstructure and transform partially to martensite on deformation. These steels are hardened considerably by cold deformation. Other commercially available austenitic stainless steel contain up to around 0.2% nitrogen. These steels are no longer unstable under deformation and therefore do not work harden to the same extent, but the austenite is itself strengthened by the nitrogen.[2] The material specification for Type 304 stainless steel is shown in the following table. Note the minimum Charpy V-Notch (CVN) absorbed energy is 100 joules.

Table 1
Material Specification for Type 304 Stainless Steel

Material	Cr	Ni	C	0.2% Sy (MPa)	Su (MPa)	Charpy (J)
304	19	9	<0.08	240	590	100 min

FACTORS AFFECTING CRYOGENIC STRENGTH & TOUGHNESS IN WELD METAL

Generally the toughness in austenitic stainless steel weld metal at cryogenic temperature is significantly lower than the base metal. Metallurgical factors causing low toughness in weld metal are well known to be precipitates such as carbides, nitrides, and intermetallic compounds. The presence of delta ferrite and non-metallic inclusions are also well known detractors to toughness. Weld toughness is affected by many factors. The effect of strength is shown in Figure 1. Toughness is adversely affected by increasing strength. However, weld material has always had a lower toughness than wrought material.

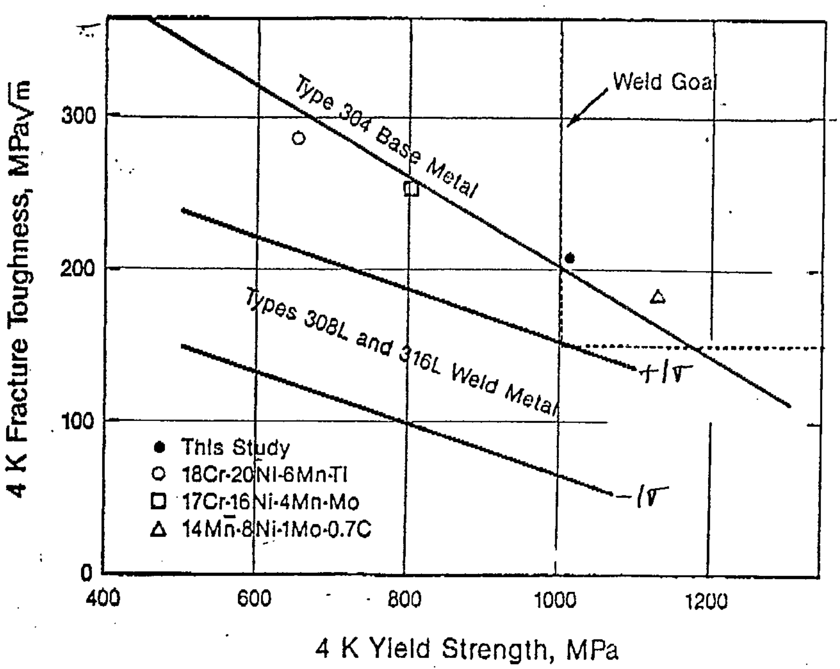

Figure 1
Comparison of the Weld and Base Metal Strength-Toughness Relationship

Nitrogen

The strengthening characteristics of nitrogen become more evident at lower temperatures. Figure 2 shows how 316L weld strength increases by a factor of 2 as temperature is decreased from 298k to 76K, and increases by a factor of 2.5 at 4K for the same 0.20% nitrogen. But varying nitrogen from 0.05% to 0.20% at 4K yields a three-fold increase in strength.

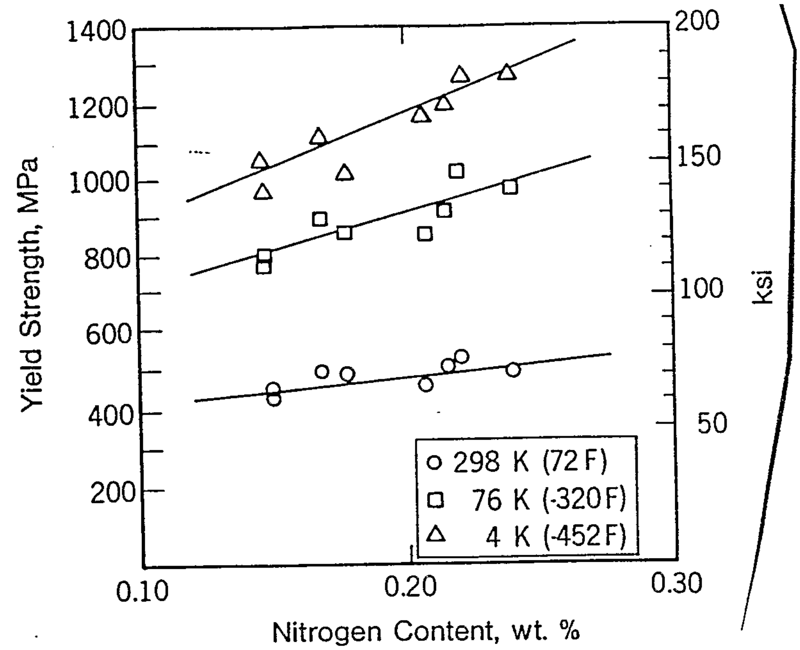

Figure 2
Yield Strength versus Nitrogen Content for Type 316LN Welds

This is most graphically demonstrated by the following equation developed by Simon and Reed[3] for Type 316 weld deposits at 4K:

$$\sigma_Y(MPa) = 316 + 2370N + 54Mo + 790d^{-1/2}$$

where N and Mo are in weight percent and d is the grain size in micrometers. The standard deviation of the data for this fit was 40 MPa. Similarly for Type 304 welds at 4K:

$$\sigma_Y(MPa) = 180 + 3200N + 33Mo + 32Mn + 13Ni$$

where the standard deviation was found to be 31MPa. The strength prediction is nearly equal for compositions near 18Cr-8Ni, indicating base metal and weld strengths are controlled by the same metallurgical phenomena.

Oxygen

Weld material has always had a lower toughness than wrought material. The difference between weld material and wrought material are the inclusion and ferrite contents. Welds will have a higher inclusion content because of the imperfect gas shielding of the metal while molten. Studies have shown that toughness correlation with inclusion spacing is similar for wrought material, thus attributing the differences in fracture toughness to this one factor[4]. Therefore choosing the welding process that produces the lowest inclusion content or modifying the process to reduce inclusion content are required to improve weld toughness.

Welding processes such as laser, electron beam and gas tungsten arc welding (TIG) can produce welds with lower inclusion contents and produce welds with toughness at the upper side of the scatter band[5] (Figure 1).

Other testing[6] has been conducted using 308, 308L, and 316L filler metal, TIG with 100% Ar shielding or gas metal arc welding (MIG) with Ar/2%O and Ar/5%O, and 304 or 317LN base plates. The results are shown in Figure 3. Calculated ferrite number for the 316L welds from the DeLong diagram was about 7%. Measured ferrite numbers for 316L weldment were 9% using TIG and 8% using MIG. Chemical composition was consistent using the different processes, but differed drastically in oxygen content (0.005 - 0.076). Lateral expansion properties would meet ASME requirements at 173K but only the TIG weld shielded with pure Ar would meet the requirement at 77K. Impact energies at 4K were also significantly affected by oxygen content despite an observed decrease in strength at 4K due to oxygen.

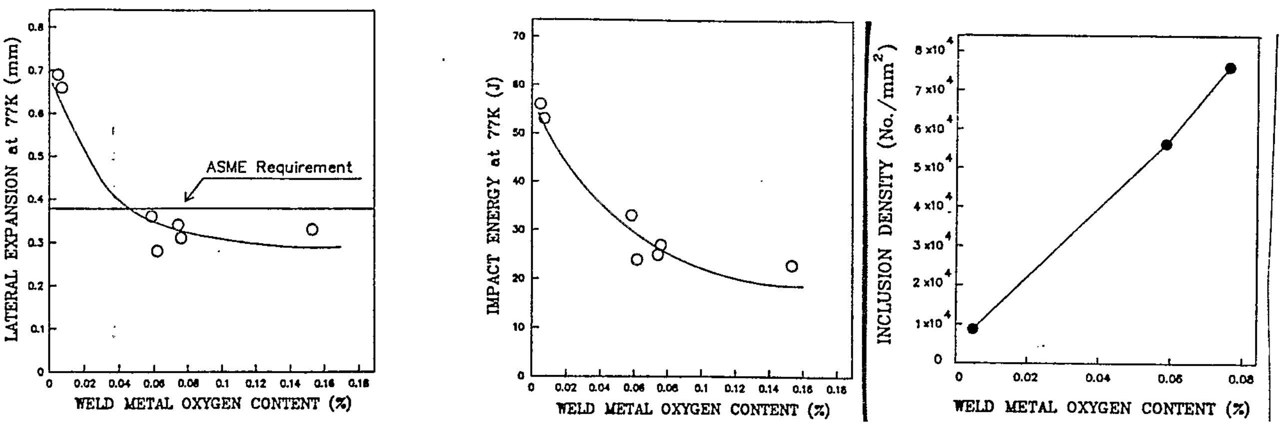

Figure 3
Results of Oxygen Content Investigation[6]

Measured ferrite number for 308/308L welds ranged from 5 to 18%, and oxygen content ranged from 0.007 to 0.15%. 308/308L welds were similarly affected by oxygen content with steep declines in lateral expansion and impact energy. Impact properties began to stabilize when oxygen content reaches 0.06% oxygen.

Testing revealed a relationship between ferrite number and oxygen content for meeting the ASME lateral expansion requirement. However, it was found that the low oxygen TIG weld could meet the ASME requirement quite safety even with a relatively high ferrite content, while the high oxygen content welds cannot meet the lateral expansion requirement even with a ferrite number of just 5%. This accounts for the ASME recommendation for a ferrite number lower than 3 for weldments other than TIG.

The study by J.H. Kim also found an excellent correlation between lateral expansion and impact energy at 173K and 77K. This relationship is described by:

$$LE(mm) = 0.12 \times C_V (Joule)$$

Thus, the ASME lateral expansion requirement is equivalent to an impact energy of 32 joules (23.6 ft-#).

Fractographic analysis of the 77K Charpy V-Notch specimens revealed increased brittleness with decreased oxygen content. This is attributed to retained delta-ferrite. Thus fracture will follow the brittle ferrite phase, but the whole fracture process requires high energy for continuous brittle fracture in the tough austenite matrix. High oxygen welds initiate by micro voids and propagate by micro void coalescence so easily that the whole fracture occurs in a fully dimple mode at low energy. Therefore it is possible to increase impact toughness in low oxygen welds by decreasing ferrite, but ferrite control would not be effective in high oxygen welds because ferrite has a negligible role in the fracture process.

This effect was also studied by Whipple and Kotecki[7] who produced a series of 316L welds using TIG, MIG, and Shielded Arc. The toughness at 4K was found to be inversely proportional to the inclusion content, with the highest toughness found in the TIG welds (181 MPa).

Other research[8] found the 4K K_{Ic} of Type 316L stainless steel weld composition increased significantly when inclusion contents in MIG welds were decreased. The study showed an increase of 18 MPA$\sqrt{m}$ per micron increase in average inclusion spacing. Other studies have shown that toughness increases with Ni content and decreases with increasing strength and inclusion content. This, then, accounts for the lower toughness in welds when compared to base metals of comparable strength and Ni content. T.A. Siewert and C.N. McCowan's study[8] used specimens made from one inch thick welds formed by multiple passes using varying shielding gas composition over 304 plate with 316L electrode. The electrode composition was 0.02 C, 1.73 Mn, 0.35 Si, 0.008 P, 0.009 S, 19.2 Cr, 13.1 Ni, 2.15 Mo, and 0.04 Cu. The ferrite number of the welds ranged from 5 to 7 measured in accordance with ANSI/AWS Standard 4.2-74. Material properties are shown in Table 2. One may see the inclusion density had little effect on yield strength, which varied less than 4%, but there is a trend toward decreasing ductility with increasing inclusion content. Note, too, the K_{Ic} values and how they compare with the K_{Ic} value of 151 MPa$\sqrt{m}$ calculated using the equation below. Clearly, minimizing inclusions will assure minimum toughness properties. Inclusions were spherical $MnSiO_3$ type inclusions with diameters less than 1 µm. The strain testing revealed heavy surface textures during straining at 4K. This is attributed to the coarse dendritic crystal structure of welds, and can result in stress concentrations that initiate failure. Note that fracture toughness increased by 35% as the inclusion content decreased by 65%. It is concluded that the wide scatter for toughness property data of weld metals are attributed to the varying inclusion contents when several welding processes are used.

Table 2
Inclusion Effect on Impact Toughness[8]

σ_y	%El	%Ra	K_{Ic}	O_2 wt %	Inclusions per mm^2	Inclusion spacing (µm)
736	47.9	46.6	179	0.004	19,300	7.0
747	22.3	23.7	150	0.048	37,700	5.0
743	10.2	13.1	132	0.072	55,200	4.3

Fractographic examination of CVN specimens revealed smaller void sizes in the cross sections of the tension specimens when compared to the ductile dimple sizes on their fracture surfaces. This implies that the dimple growth process is caused by local flow during fracture. Voids, however, were observed to be linked by crack-like features. Voids nucleated at inclusions near the ferrite-austenite interface to form the intervoid cracking. Cracking in the ferrite or at the ferrite-austenite interface was not observed in this study.

Ferrite

Toughness is usually measured by energy absorption or lateral expansion during a Charpy V-Notch (CVN) test and is widely used at 76K as a screening test. Studies have shown that CVN can be predicted for 76K with a 95% confidence level by the formula:

$$CVN(J) = 19 - 1.4FN - 890C^2 + 1.4Ni$$

where FN is the ferrite number calculated by the Schaeffler Diagram, and C and Ni are by weight percent. This relationship demonstrates the deleterious effects FN and carbon have on impact energy, while nickel has a positive influence. Ferrite content is especially important. Ferrite occurs when the composition is adjusted to develop metastable austenite. Ferrite in small quantities is normally desirable in stainless steels welds because it inhibits the formation of low melting point compounds (such as FeS and FeP) that promote hot cracking in fully austenitic alloys. However, ferrite should be minimized for best toughness in cryogenic service. Therefore, welding alloys for cryogenic service are either ferrite-free or very low ferrite. The ferrite-free alloys are produced with very strict controls on the impurity contents that promote hot cracking.

Nickel

Nickel also has a significant, though non-linear, effect on toughness. Figure 4 shows that increasing nickel from 10% to 20% provides the greatest improvement in toughness. Thus a weld with 20% nickel should exhibit the greatest attainable toughness for an austenitic stainless steel. NIST had performed work to determine the best weld material for 316LN, which is recognized as the candidate material for demanding cryogenic applications[9]. Two commercially available compositions - 18Cr-20Ni-5Mn-0.16N and 20Cr-25Ni-4.5Mo were evaluated using gas metal arc welding. Inerting gases were more inert than normal to reduce oxygen content, and the gas used for the 20Cr-25Ni-4.5Mo electrode was augmented with nitrogen to increase the nitrogen in the weld metal. Figure 5 shows that the strength was comparable to 316LN base metal and the fracture toughness was as high as or exceeded that of the 316LN base metal. This toughness is clearly higher than the toughness achievable with 308 and 316-based welding compositions and standard welding procedures.

Manganese[10]

Significant testing and statistical analysis was conducted on Type 308 and 316 weld metal applied to Type 304LN stainless steel plate by multilayer welding using several techniques. Impact energies for carbon steels is nearly directly proportional to the lateral expansion, and testing at 77K showed an almost linear relationship for Type 316Mn weldment. Additionally, it has been demonstrated that the relationship remains linear below 122K. The ferrite numbers measured on the test samples did not correlate with Szumachowski's constitution diagram. The results of the testing at 4.2K is provided in Table 3. Note that the Type 316 welds resulted in consistently high impact energies.

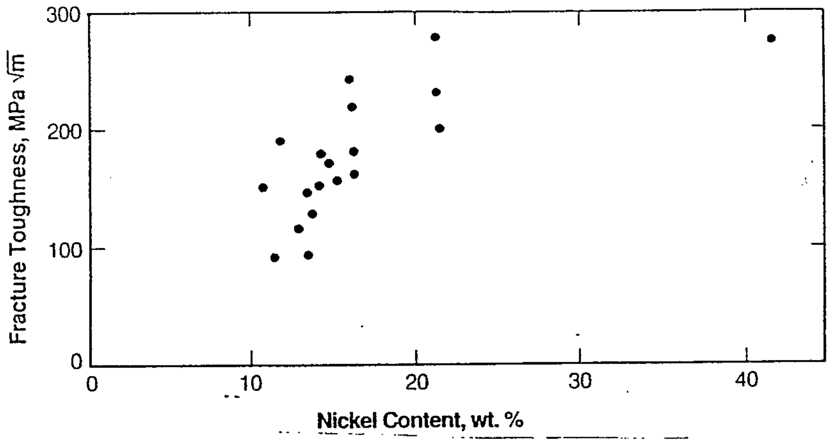

Figure 4
Fracture Toughness versus Nickel Content

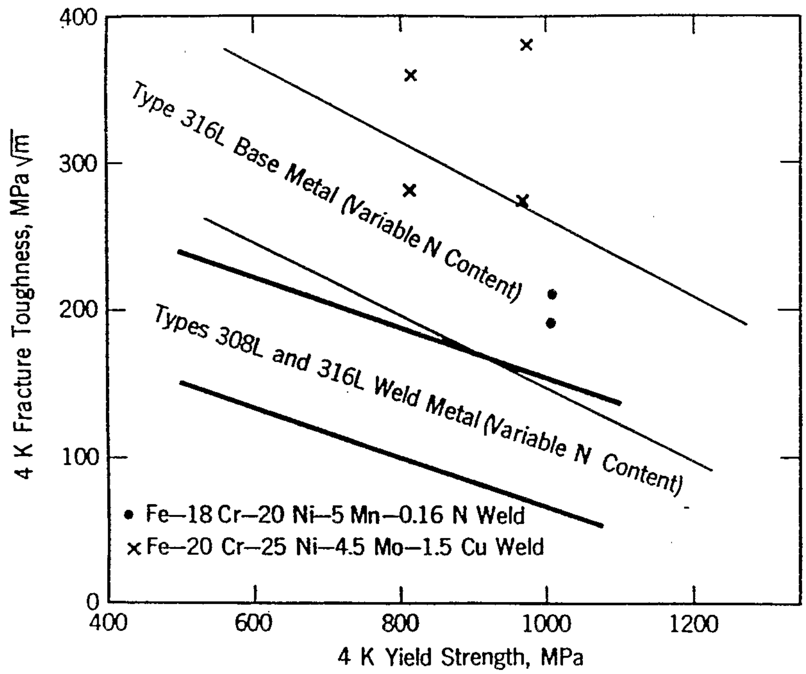

Figure 5
Fracture toughness versus Yield Strength

Table 3
4.2K Lateral Expansion and Absorbed Energy

Type Filler	Weld Process	Electrode Diameter	Lateral Expansion	Impact Energy (J)
308Mn	TIG	5 mm	0.31 mm (0.012 in)	29(J) (21.4 ft#)
308Mn	MIG	1 mm	0.53 mm (0.021 in)	68(J) (50.2 ft#)
308N	TIG	4 mm	0.10 mm (0.004 in)	9(J) (6.6 ft#)
308N	MIG	1.6 mm	0.06 mm (0.002 in)	7(J) (5.2 ft#)
316Mn	TIG	2.4 mm	1.08 mm (0.043 in)	80(J) (59.0 ft#)
316Mn	MIG	1.2 mm	1.12 mm (0.044 in)	78(J) (57.5 ft#)

Through multiple regression analysis, a prediction formula for absorbed energy at 4.2K was found to be:

$$vE = 90.6 - 4.56(FN) - 44.2(\%C) - 824(\%O).$$

Note that this study also found oxygen content to be a significant detractor to fracture toughness. Testing found that calculated ferrite number was only reliable if a ferrite indicator or Magne Gage did not detect ferrite. If ferrite was not detected, ferrite number was calculated using a modification of the Ni equivalent for the Szumachowski's constitution diagram. If ferrite was detected, then measured ferrite is used in the prediction equation. This report did not consider the effects of welding conditions nor post weld heat treatment. The predictions were found to be within five joules of the test data.

Ferrite

Weld compositions may vary widely within the broad but clearly specified compositional ranges for Types 308 and 316 weld metal. Weld metals with unrestricted compositions have been developed for cryogenic service, including some with high manganese contents. Weld microstructure is determined by composition. It can be single phase (fully austenitic) or two-phase (austenite and delta-ferrite) with ferrite number (FN) up to 12. Type 308L and 316L weld compositions usually contain a small amount of ferrite to prevent fissuring. Unrestricted compositions are more resistant to fissuring and do not contain ferrite. NIST data show an inverse relationship between yield strength and fracture toughness . Welds with FN>7 show relatively low toughness, but welds with lower FN contents fall randomly within the one sigma scatter band of +/- 44MPa[11]. This is shown graphically in Figure 1. Thus ferrite should be reduced to the lowest level consistent with fissure resistance.

Austenitic stainless steel welds generally fail by a ductile fracture mechanism typified by the formation and growth of voids that eventually compose the fracture surface. Therefore, toughness improvements must increase the resistance of the weld metal to the nucleation and growth of voids. Voids nucleate most readily near phase boundaries, as a result of interfacial separation, fracture within the second phase, or matrix separation caused by strain concentration. Hence toughness may be improved by eliminating or minimizing other phases such as delta ferrite, chromium carbides, and inclusions.

The growth and coalescence of voids relates to the strength, ductility, and strain-hardening behavior of the matrix. As matrix strength increases, less energy is dissipated by plastic deformation during void growth, thus reducing toughness. Increased matrix strength also tends to activate additional void nucleation sites, hence alloying with interstitial elements such as carbon and nitrogen tends to reduce fracture toughness.

Test data available to date indicates the strength-toughness characteristics of welds may be increased by eliminating delta ferrite, avoiding chromium carbides, and reducing the width of columnar grains. These actions will raise the trend line of the weld strength-toughness characteristics closer to that of wrought stainless steel.

Relationship between Yield Strength and K_{Ic}

The National Institute of Standards and Technology (formerly National Bureau of Standards) has been compiling cryogenic mechanical property data for structural alloy welds for 4K service for the past two decades. Their work to date demonstrates[12]:

1) there is an inverse correlation between yield strength and fracture toughness for stainless steel welds at 4K, and

2) The welds have significantly lower toughness than base metals of comparable strength

The toughness of Types 308L and 316L welds is described by:

$$K_{I_c}(MPa\sqrt{m}) = 270 - 0.16\sigma_y(MPa)$$

For AISI Type 304 austenitic stainless steels with varying carbon and nitrogen contents, the empirical relationship is given by:

$$K_{I_c}(MPa\sqrt{m}) = 500 - 0.3\sigma_y(MPa)$$

One may see the obvious disparity between the equations for welds and base metal. Welds generally fall about 40% below base metals in their σ_y versus K_{Ic} performance (See also Figure 1).

Charpy Impact Testing for Determining 4K Toughness

Charpy V-Notch impact testing (CVN) at the operational temperature is required to ensure the toughness of materials by the ASME Boiler and Pressure Vessel Code and the Japanese Industrial Standards Pressure Vessel Code, among others. There are two methods for conducting 4K Charpy tests. One method uses a sacrificial glass dewar. This method requires a correction factor to account for the energy required to break the glass and the gap between the glass and the specimen. The other method is described as the flow method, wherein the specimen is wrapped in foam and Kapton tape and liquid helium is then transferred into the envelope. The values measured by both tests correlate very well as long as the initial temperatures are the same. The correction factor from the glass dewar method can be determined at room temperature because the factors involved were found to be independent of temperature. The Charpy values should correlate with the fracture toughness parameters J_{Ic} or K_{Ic} if the Charpy tests are to be used to determine material properties. This correlation was not found for 4K tests because the specimen temperature rises significantly during 4K Charpy impact testing. The temperature rise is caused by adiabatic heating during high strain rate deformation and the low heat capacity of the material at 4K. Further study found a low correlation factor between the fracture toughness parameters and the Charpy results for the test data available for 304/308/316 materials[13]. Thus 4K Charpy tests are not a reliable indicator of 4K fracture toughness.

Discussion with NIST

Mr. Siewert and Mr. Ralph Tobler, both of the National Institute of Standards and Technology [formerly NBS] were consulted directly. Mr. Siewert and Mr. Ralph Tobler have written numerous papers concerning 4K impact and fracture properties of austenitic stainless steels. About five years ago, Mr. Tobler and Mr. Siewert began separate investigation of austenitic material properties — Mr. Tobler investigated base metals and Mr. Siewert investigated weldment. Mr. Siewert was hired specifically to investigate weldment because of his background in the welding industry. Mr. Tom Siewert (303-497-3523) was consulted regarding NBS testing of austenitic weldment at 4K. Reference 12, entitled *Strength-Toughness Relationship for Austenitic Stainless Steel Welds at 4K* was received without a date . Mr. Siewert put the date at approximately 1986. Mr. Siewert has recently published a paper in the ASTM Journal of Test & Evaluation entitled *Charpy Impact Near Absolute Zero* (Vol.19, Jan 1991; pp. 34-40)[copy provided]. The paper summarizes the NBS testing for the past 15 years regarding austenitic weldment at 4K. He generally discussed several aspects of austenitic weldment at 4K. The following is a summary of his comments:

- Type 316 and type 308 are both compatible with 304 plate. NIST's recommendation has been to use 316 for welding 304 for cryogenic applications.
- Type 316 weld material has demonstrated superior material properties at cryogenic temperatures, hence NIST testing for the past 5 years has concentrated on that type.
- Type 316 has more nickel giving it much better impact properties and making it much more fissure resistant, thus minimizing hot cracking. The 10% increase in cost is insignificant when compared to the gain in material toughness.
- NIST had done some work for SSC. Apparently SSC had wanted to use nitronic for beam tube. He said nitronic is terrible material for cryogenic applications because of the very low toughness despite the great "book" strength. NIST recommended 316.
- Mr. Siewert was asked why all NIST testing concentrated on developing impact energy when the ASME wants to know lateral expansion for austenitic material. He said lateral expansion is of dubious merit and that the lateral expansion is a "fuzzy" property. Likewise, Charpy energy is also somewhat "fuzzy". He and the NIST have been recommending K_{Ic} be used as the governing design parameter for impact toughness.
- Mr. Siewert does not view Charpy impact energy and testing at 4K as very useful. ASTM E23 does not address it in the procedure. The testing is near impossible today to validate. During Charpy impact testing[13] the adiabatic heating of the test specimen during deformation can drive local temperatures to 200K! Thus, even if one could keep the specimen at 4K up to the moment of impact, the material would not be at 4K during the test. This is attributed to the heat capacity of the material at cryogenic temperatures. This testing may provide acceptable data for projectile impact tests; but cannot provide valid data for a large structure at 4K. Ralph Tobler (NBS) has coauthored a paper discussing this issue and Mr. Siewert provided a copy.
- Mr. Siewert is also on the ASTM Committee for Standard E23, the Charpy impact testing standard. His committee has been at odds with the ASME for the past few years. The Standard E23 is under revision now and will contain a statement that the test procedure is not valid for testing materials below 76K. He does not know what ASME will do when the ASTM standard is revised. The new standard should be issued this year.
- The RHIC dipole situation was presented to Mr. Siewert. Two 304 half shells are wrapped around a carbon steel core and then welded. Mr. Siewert said that the root of the weld would contain very high ferrite and would probably hot crack. This would be very bad from a fracture standpoint because the cracks would form initiation sites for catastrophic fracture. He recommended that an austenitic backing strip be used to prevent any ferrite formation.

Magnetic Field Effects

Magnetic effects were also researched. In short, the magnetic effects would be negligible from a fracture standpoint. A more detailed discussion is provided in Appendix A.

FRACTURE MECHANICS ANALYSIS

Fracture mechanics analysis was conducted to the greatest extent possible. Some data is either not available or is grouped together with weld processes and/or materials that are not applicable to the RHIC dipole longitudinal weld situation. The applicability of the fracture mechanics formulae was validated by:

$$B \geq 2.5\left(\frac{K_{Ic}}{\sigma_y}\right)^2$$

where B is material thickness

The resultant found the thickness of the coldmass shells exceeded the minimum thickness required for plain strain conditions for K_{Ic} below 50 MPa√m.

Fracture Mechanics Design Criteria

Fracture mechanics design criteria were also evaluated. These consist of the Through-Thickness-Yielding criterion and the Leak-before-Break criterion. Through-Thickness-Yielding means that in the presence of a large sharp crack in a large plate, through-thickness-yielding should occur before fracture. Leak-before-Break means that a surface crack should grow through the wall thickness of the vessel and leak before the vessel fails by fracture. Calculations were performed using the NIST relationship between K_{Ic} and σ_y and by iterating K_{Ic} over a range for expected values of σ_y at 4K. These calculations indicate σ_y must be about 1100 to 1200 MPa with a corresponding K_{Ic} of 94 MPa√m for K_{Ic} as a function of σ_y. This is not likely considering the average 4K σ_y for 308/316 welds being between 700 - 800 MPa. Thus K_{Ic} should have the minimum values indicated in Table 5. The calculations are provided in Appendix B.

Table 5
Minimum K_{Ic} Required at 4K for Various Yield Strengths

Yield Strength (MPa)	700	800	900	1000
K_{Ic} (Leak-before-Break)(MPa√m)	60	68	77	85
K_{Ic} (Through-Thickness-Yielding)(MPa√m)	49	56	63	70
K_{Ic} (Calculated from σ_y)(MPa√m)	158	142	126	110
K_{Ic} (Calculated - 2sd)(MPa√m)	70	54	38	22

It would appear that the welds would possess more than adequate fracture toughness. However, the calculated K_{Ic} has a standard deviation of 44 MPa√m. Thus the welds would have marginal fracture toughness for a confidence factor of only 95% for the 700 - 800 MPa 4K yield strength range (Calculated K_{Ic} - 2sd in Table 5).

Fracture mechanics analysis also was conducted to determine the critical crack size. In fracture mechanics design, critical defect size is required to establish quality controls to prevent the critical size defect from occurring or going into service. The calculations considered a through thickness crack of width 2a, and a semi-elliptical shaped surface defect measuring 'a' in depth and 2c wide. These calculations are contained in Appendix C. Sensitivity study reveals higher K_{Ic} is required as the crack width (2c) becomes very large in comparison to the crack depth (a). The equation for K_{Ic} for a surface crack is prescribed by

$$K_{Ic} = 1.12\sigma_y\sqrt{\frac{\pi a}{Q}}$$

where:

$$Q = \left[\Phi_o^{\ 2} - \left(0.212\left(\frac{\sigma}{\sigma_y}\right)^2\right)\right]$$

and Φ_o is the elliptical integral. Iterating over a range of crack depths (a) and stress ratios (σ/σ_y), the worst case for a surface crack with depth equal to the shell thickness and width 20 times the shell thickness requires a K_{Ic} of 56 MPa$\sqrt{}$m.

Similar calculations were conducted for a through thickness crack. Maximum critical defect size is shown in Figure 6. This demonstrates the significance of K_{Ic}. These calculations also are contained in Appendix C.

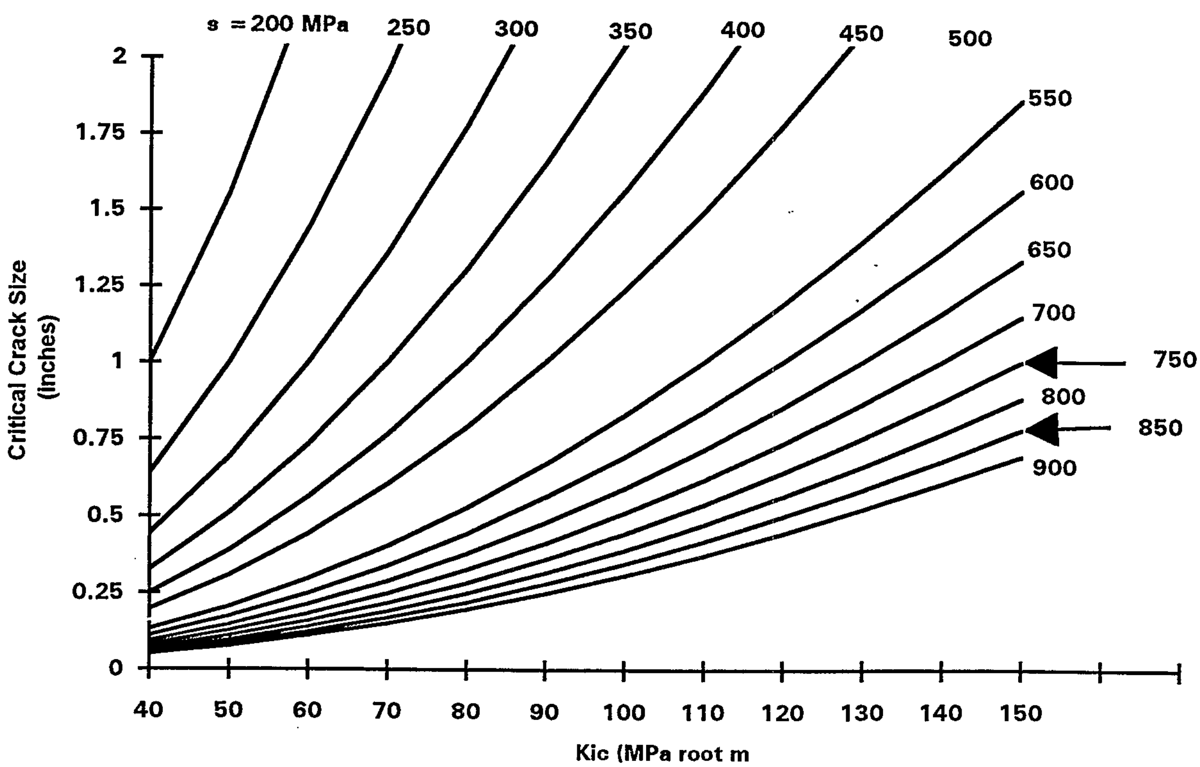

Figure 6
Critical Crack Size for Various K_{Ic} and Material Stresses

Finally, it has been previously established that a Charpy absorbed energy of at least 32 joules is necessary to meet the ASME minimum lateral expansion of 0.015 inches (0.38 mm).

Reference 9 provides an equation for 76K CVN as a function of ferrite number, calculated from the Schaeffler Diagram (ferrite potential if negative), carbon content, and nickel content.

$$CVN\,(J) = 19 - 1.4FN - 890C^2 + 1.4Ni$$

This equation was iterated for several expected values for FN, C, and Ni. The results, contained in Appendix D, indicate that a CVN of 32 joules is not possible with FN greater than 2, C greater than 0.03%, and Ni less than 12%. This equation obviously does not address the oxygen content previously discussed.

Discussion of Fracture Mechanics Analysis

The analysis shows that 308L/316L weld material nominal 4K mechanical properties exceed fracture mechanics design criteria. The data scatter, however, would require a weld with nominal properties at the upper band shown in Figure 1. This is possible with TIG welding, or by using other compositions, namely 18Cr-20Ni-5Mn-0.16N (Figure 5). This should be sufficient to negate the ASME requirement for 4K impact testing when considering the questionable outcome of the 4K testing and the fact that the ASTM Standard will be changed in the near future to limit the applicability of the procedure only down to 76K. Testing in the last few years has shown that austenitic stainless steel properties at 4K do not exhibit a detrimental decrease in fracture toughness. Since the ASME already allows the use of these materials to 20K without the need for impact testing, RHIC should not be at risk by not requiring impact testing for materials operating at 4K. However, the issue becomes that of quality controls. Maximum defect size has been calculated, but there is no procedure in place to detect these defects. MIG welding is also questionable. Clearly TIG welding offers the best assurance that the inclusion content has been minimized, but there needs to be some type of testing to validate the chemical composition, particularly with regard to ferrite number, carbon, nickel, sulfur, phosphorous, and oxygen regardless of welding process. This would apply to the filler material and a sample of the finished weld. The impact test was developed as some relatively simple means for verifying all these requirements. If the establishment of the quality controls is considered to onerous, perhaps a 76K impact test should be considered. Another investigation would be required to determine the necessary impact value at 76K to assure 4K properties. RHIC also may consider leaving this effort up to the dipole contractor, as some of the candidates have qualified fracture mechanics and weld engineering departments. Finally, all these discussions and data apply to uncontaminated weld metal, or weld metal applied to austenitic stainless steel plate. The deleterious effects of carbon and ferrite have been thoroughly discussed here. The weld testing performed by C. Czajkowski[14] was only qualitative in nature, but was able to show significant magnetization of the weld root material. Since we know the ferrite number for 308 weld metal must be at least 5 -18%, the weld root for the tested weld must have a significantly higher ferrite number, Thus it cannot possess adequate fracture toughness.

CONCLUSIONS

This research leads to several conclusions.

1) Impact testing at 4K does not yet provide consistent results. It may be difficult to impose 4K impact testing on a contractor because the ASTM standard will not be applicable to temperatures below 4K. Impact testing also will be complicated because of the difficulty in obtaining a sample with contamination representative of the actual coldmass longitudinal welds.
2) The preferred weld metal for 4K applications is Type 316L. Some other materials offer superior fracture toughness at similar 4K yield strengths, such as 18Cr-20Ni-5Mn-0.16N.
3) The preferred weld processes for 4K applications are laser, electron beam, and TIG.
4) Type 316L will have sufficient fracture toughness thereby exceeding the ASME requirements if the oxygen content is minimized. This cannot be achieved with conventional MIG processes.
5) Other quality controls must be imposed if impact testing will not be conducted, especially for a contaminated weld root. These controls must be capable of detecting critical flaw size and chemical composition, particularly with regard to ferrite number, carbon, nickel, sulfur, phosphorous, and oxygen.
6) In all likelihood, it probably will not be possible for the weld root material to meet the fracture toughness criteria, especially with respect to ferrite number. The high stresses in the longitudinal weld will exacerbate the fracture toughness problem because of the additional martensitic transformation potential and the higher stress/yield stress ratio.
7) The incorporation of an austenitic stainless steel backing strip of sufficient thickness to prevent contamination of the weld material will minimize the quality controls necessary to assure weld fracture toughness. The use of the TIG weld process will probably reduce the requirement for quality controls to verification of oxygen content. This will be relatively easy to accomplish if the backing strip is used, thus assuring uncontaminated weld material in the sample as well as making the sample representative of the actual weld.

References:

[1]R.P. Reed, Acta Mettalica 10, 865, 1962

[2]U.R. Lenel and B.R. Knott, Metallurgical Transactions A, Vol.18A, May 1987 (847)

[3]N.J. Simon AND R.P. Reed, NBSIR 88-3082, National Bureau of Standards, Gaithersburg, MD; 71 (1988)

[4]T.A. Siewert and C.N. McCowan; Advances in Cryogenic Engineering (Materials), Vol. 38b, 1992, 109

[5]T.A. Siewert, D. Gorni and G. Kohn; Advances in Cryogenic Engineering (Materials), Vol. 34b, 1988, 343

[6]J.H. Kim, B.W. Oh, J.G. Youn, G. Bahng, and H. Lee, Advances in Cryogenic Engineering (Materials), Vol. 36B, 1990

[7]T.A. Whipple and D.J. Kotecki, NBSIR 81-1645, National Bureau of Standardddds, Boulder, CO (1981) 303

[8]C.N. McCowan and T.A. Siewert, Advances in Cryogenic Engineering (Materials), Vol. 36b, 1990, 1331

[9]T.A. Siewert and C.N. McCowan; NISTIR 3944, 1990 (233); and T.A. Siewert, R.L. Tobler and C.N. McCowan; Journal of Engineering Material and Technology 108, 1986 (340)

[10]T.Mori and T. Kuroda, Cryogenics 25:243, 1985

[11]D.T. Reed, H.I. McHenry, P.A. Steinmeyer, R.D. Thomas, Jr., Welding Journal 59, 1980, 104

[12]R.L. Tobler, T.A. Siewert, and H.I. McHenry; Cryogenics, 1986

[13] H. Nakajima, K. Yoshida, H. Tsuji, R.L. Tobler, I.S. Hwang, M.M. Morra, and R.G. Ballinger; International Cryogenic Materials Conference, Huntsville, AL, 11-14 June 1991 (FZ-6)

[14]C. Czajkowski BNL Memorandum to M. Linden, Subject: Magnetic Evaluation of Two Stainless Steel Welds, 31 January 1991

APPENDIX A

Discussion of Magnetic Effects

MAGNETIC FIELD EFFECTS

An increase in the fracture toughness of 304 specimens tested at 4.2K in an 8T magnetic field is observed relative to the fracture toughness of specimens tested in 0T. This increase is partly ascribed to the differences in martensitic transformation ahead of the crack tip during the Jic tests[15]. The characterization problem is complex because these metastable austenitic steels can undergo strain-induced martensitic transformation at cryogenic temperatures. Permeability measurements showed high permeability α' phase forms near the fracture surface and decreases with distance from the fracture surface. The amount and extent of α' formation was qualitatively larger for the specimens tested in the 8T field. Various studies of the effects of pulsed and steady magnetic fields on the martensitic behavior of steels of various compositions found the amount of transformations was shown to be enhanced in the presence of a field. The extent of transformation was shown to be a function of field strength and independent of frequency and number of applied pulses. The volume of ferromagnetic α' formed during deformation in a magnetic field has a direct effect on the crack tip stress intensity. The plates would tend to resist separation in a measurable fashion since the magnetic flux is contained within the ferromagnetic material. The formation of martensite around the crack creates a closing load on the crack during Jic tests on CT specimens in a solenoid field with the loading direction parallel to the solenoid axis. The magnitude of this effect was found to be approximately a 1 MPa m1/2 reduction in crack tip stress intensity, representing a 2 - 3% improvement if measured fracture toughness. Testing has also shown that 304L and 304LN had higher strain hardening rates when tested in an applied field[16].

---

[15] J.W. Chan, J. Glazer, Z. Mei, and J.W. Morris, Jr.;4.2K Fracture Toughness of 304 Stainless Steel in a Magnetic Field; Advances in Cryogenic Engineering - Materials, Vol. 36B, 1989

[16].B Fultz and J.W. Morris, Jr., Acta Mettalica, 34:379, 1986

APPENDIX B

Calculations for Leak-Before-Break and Through-Thickness-Yeilding

crack5.mcd

This calculates leak before break and through thickness yield before fracture criteria. These calculations assume the weld is the weak link and the weld material follows the relationship defined by KIC = 270 - 0.16 σy.

leak-before-break criteria

$B := 4.763 \cdot 10^{-3}$ Dipole shell thickness in meters

$s := 100, 200 .. 1200$

$$F(s) := \frac{1.4 \cdot \left[(270 - (0.16 \cdot s))^6\right]}{B^3 \cdot s^4} + \frac{(270 - (0.16 \cdot s))^2}{B}$$

$$G(s) := 2 \cdot \pi \cdot s^2$$

G(s)	F(s)
$6.28319 \cdot 10^4$	$3.47928 \cdot 10^{13}$
$2.51327 \cdot 10^5$	$1.47174 \cdot 10^{12}$
$5.65487 \cdot 10^5$	$1.91488 \cdot 10^{11}$
$1.00531 \cdot 10^6$	$3.86856 \cdot 10^{10}$
$1.5708 \cdot 10^6$	$9.76035 \cdot 10^9$
$2.26195 \cdot 10^6$	$2.78081 \cdot 10^9$
$3.07876 \cdot 10^6$	$8.44772 \cdot 10^8$
$4.02124 \cdot 10^6$	$2.63566 \cdot 10^8$
$5.08938 \cdot 10^6$	$8.23536 \cdot 10^7$
$6.28319 \cdot 10^6$	$2.54936 \cdot 10^7$
$7.60265 \cdot 10^6$	$7.96009 \cdot 10^6$
$9.04779 \cdot 10^6$	$2.68446 \cdot 10^6$

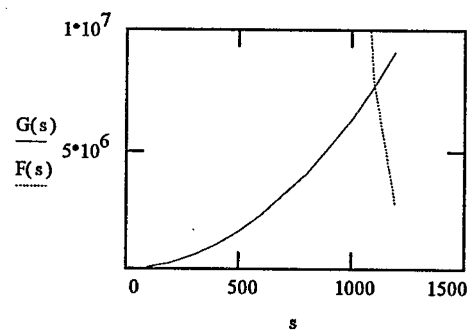

$s := 1103.476$

$G(s) = 7.65078 \cdot 10^6$ $F(s) = 7.65078 \cdot 10^6$

$Kc(s) := 270 - (0.16 \cdot s)$

$Kc(s) = 93.44384$

Through-Thickness-Yielding Criteria

$B := 4.763 \cdot 10^{-3}$ Dipole shell thickness in meters

$s := 1100, 1110 .. 1200$ $Kc(s) := 270 - (0.16 \cdot s)$

$K(s) := s \cdot \sqrt{B}$ $B = 0.00476$

Kc(s)	K(s)
94	75.91594
92.4	76.60609
90.8	77.29623
89.2	77.98638
87.6	78.67652
86	79.36666
84.4	80.05681
82.8	80.74695
81.2	81.4371
79.6	82.12724
78	82.81739

s
$1.1 \cdot 10^3$
$1.11 \cdot 10^3$
$1.12 \cdot 10^3$
$1.13 \cdot 10^3$
$1.14 \cdot 10^3$
$1.15 \cdot 10^3$
$1.16 \cdot 10^3$
$1.17 \cdot 10^3$
$1.18 \cdot 10^3$
$1.19 \cdot 10^3$
$1.2 \cdot 10^3$

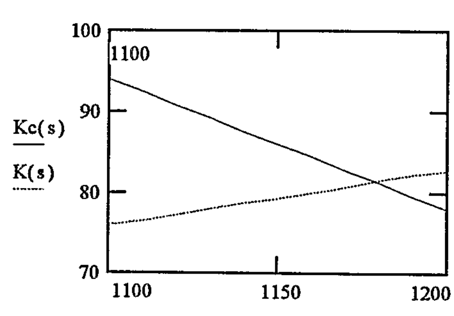

crack7.mcd

This calculates leak before break and through thickness yield before fracture criteria. These calculations assume the weld is the weak link and the weld material follows the relationship defined by KIC = 270 - 0.16 σy.

leak-before-break criteria

$B := \frac{0.1875}{39.37}$ Dipole shell thickness in meters

$K := 60, 62.5 .. 90 \quad s := 700, 800 .. 1000$ $B = 0.00476$ parameter check

$F(K,s) := \frac{1.4 \cdot \left[(K)^6\right]}{B^3 \cdot s^4} + \frac{(K)^2}{B}$

$G(s) := 2 \cdot \pi \cdot s^2$

G(s)

$3.07876 \cdot 10^6$
$4.02124 \cdot 10^6$
$5.08938 \cdot 10^6$
$6.28319 \cdot 10^6$

F(K, 700)	F(K, 800)
$3.27437 \cdot 10^6$	$2.23218 \cdot 10^6$
$4.03763 \cdot 10^6$	$2.7062 \cdot 10^6$
$4.95821 \cdot 10^6$	$3.27352 \cdot 10^6$
$6.06234 \cdot 10^6$	$3.94953 \cdot 10^6$
$7.3795 \cdot 10^6$	$4.75149 \cdot 10^6$
$8.94259 \cdot 10^6$	$5.6987 \cdot 10^6$
$1.07883 \cdot 10^7$	$6.81265 \cdot 10^6$
$1.29572 \cdot 10^7$	$8.11715 \cdot 10^6$
$1.54942 \cdot 10^7$	$9.63852 \cdot 10^6$
$1.84488 \cdot 10^7$	$1.14058 \cdot 10^7$
$2.18754 \cdot 10^7$	$1.34507 \cdot 10^7$
$2.58333 \cdot 10^7$	$1.58083 \cdot 10^7$
$3.03877 \cdot 10^7$	$1.85165 \cdot 10^7$

F(K, 900)	F(K, 1000)
$1.67754 \cdot 10^6$	$1.36059 \cdot 10^6$
$1.99763 \cdot 10^6$	$1.59271 \cdot 10^6$
$2.37695 \cdot 10^6$	$1.8646 \cdot 10^6$
$2.8251 \cdot 10^6$	$2.18256 \cdot 10^6$
$3.35288 \cdot 10^6$	$2.55365 \cdot 10^6$
$3.97233 \cdot 10^6$	$2.9858 \cdot 10^6$
$4.69685 \cdot 10^6$	$3.48778 \cdot 10^6$
$5.54132 \cdot 10^6$	$4.06937 \cdot 10^6$
$6.52217 \cdot 10^6$	$4.74134 \cdot 10^6$
$7.6575 \cdot 10^6$	$5.51556 \cdot 10^6$
$8.96719 \cdot 10^6$	$6.40509 \cdot 10^6$
$1.0473 \cdot 10^7$	$7.4242 \cdot 10^6$
$1.21988 \cdot 10^7$	$8.5885 \cdot 10^6$

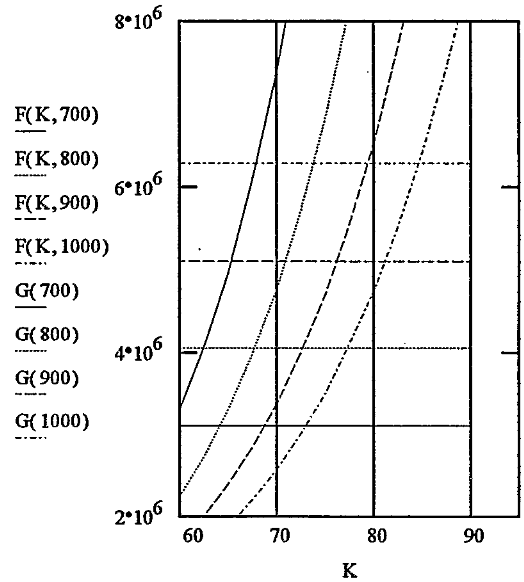

$s := 700 \quad K := 59.275 \quad Kc(s) := 270 - (0.16 \cdot s)$

$G(s) = 3.07876 \cdot 10^6 \quad F(K,s) = 3.07905 \cdot 10^6 \quad Kc(s) = 158$

$s := 800 \quad K := 67.7453 \quad Kc(s) := 270 - (0.16 \cdot s)$

$G(s) = 4.02124 \cdot 10^6 \quad F(K,s) = 4.02235 \cdot 10^6 \quad Kc(s) = 142$

$s := 900 \quad K := 76.2095$

$G(s) = 5.08938 \cdot 10^6 \quad F(K,s) = 5.08945 \cdot 10^6 \quad Kc(s) = 126$

$s := 1000 \quad K := 84.677$

$G(s) = 6.28319 \cdot 10^6 \quad F(K,s) = 6.28319 \cdot 10^6 \quad Kc(s) = 110$

Through-Thickness-Yielding Criteria

$B := 4.763 \cdot 10^{-3}$ Dipole shell thickness in meters

$s := 700, 800 .. 1000 \quad K(s) := s \cdot \sqrt{B}$

Parameter check

$B = 0.00476$

s
700
800
900
$1 \cdot 10^3$

K(s)

48.31014
55.21159
62.11304
69.01449

minimum Kic for Through-Thickness Yielding before fracture

$Kc(s) := 270 - (0.16 \cdot s)$ Kic possible at 4K with weld yield strength of 800 - 1000 MPa

Kc(s)
158
142
126
110

APPENDIX C

Calculations for Critical Crack Size and Minimum K_{Ic}

Explaination of Calculations

These calculations were performed using MathCad. The output for iterative calculations is a vertical column. If there is more than one variable upon which to iterate, MathCad fixes the second variable at its initial value, then iterates over the first variable. It then fixes the second variable at the next value in the range and again iterates over the first variable range. These successive iterations are listed consecutively in the vertical format.

crack10.mcd This file will calculate the critical crack size for various Kic, s, and crack geometries.

$a := .00047625, .0009525 .. .0047625 \quad sy := 700, 750 .. 1000 \quad s := 200, 250 .. 400$

$c(a) := a \cdot 2$

$$Q(a,c,s,sy) := \left[f(a,c)^2 - \left[.212 \cdot \left[\left(\frac{s}{sy} \right)^2 \right] \right] \right]$$

Φo $\quad f(a,c) := \int_0^{\frac{\pi}{2}} \sqrt{\left[1 - \left(\frac{c^2 - a^2}{c^2} \right) \cdot \sin(\theta)^2 \right]} \, d\theta$

$$K(a,c,s,sy) := 1.12 \cdot s \cdot \sqrt{\frac{\pi \cdot a}{Q(a,c,s,sy)}}$$

s
200
250
300
350
400

sy
700
750
800
850
900
950
$1 \cdot 10^3$

a	c(a)
$4.7625 \cdot 10^{-4}$	$9.525 \cdot 10^{-4}$
$9.525 \cdot 10^{-4}$	0.00191
0.00143	0.00286
0.00191	0.00381
0.00238	0.00476
0.00286	0.00572
0.00333	0.00667
0.00381	0.00762
0.00429	0.00857
0.00476	0.00953

Q(a,c(a),s,sy)
1.44935
1.45158
1.45341
1.45492
1.45619
1.45726
1.45818
1.43962
1.4431
1.44595
1.44832
1.4503
1.45198
1.45341
1.42772
1.43274
1.43684
1.44025
1.4431
1.44552
1.44758
1.41366
1.42049
1.42608
1.43071
1.43459
1.43788
1.44069
1.39743
1.40635
1.41366
1.41971
1.42478
1.42907
1.43274
1.44935
1.45158
1.45341
1.45492
1.45619
1.45726
1.45818
1.43962
1.4431
1.44595
1.44832
1.4503
1.45198
1.45341
1.42772

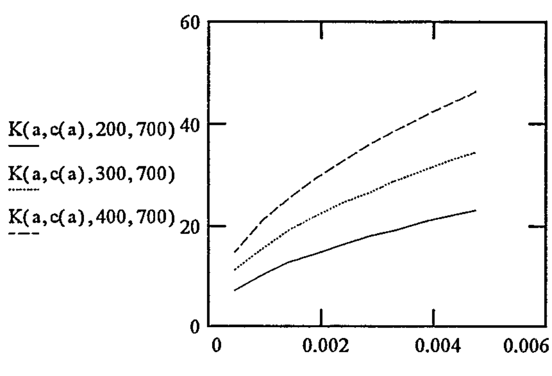

For this series of calculations, the crack is four times as wide as it is deep (4c x a) (a/2c=0.25)

K(a,c(a),s,700)	K(a,c(a),s,750)	K(a,c(a),s,800)	K(a,c(a),s,850)	K(a,c(a),s,900)	K(a,c(a),s,950)	K(a,c(a),s,1000)
7.19704	7.19151	7.18699	7.18325	7.18012	7.17748	7.17522
9.02666	9.01575	9.00686	8.9995	8.99335	8.98816	8.98373
10.87703	10.85797	10.84244	10.82961	10.81891	10.80987	10.80217
12.75283	12.72213	12.69717	12.67659	12.65942	12.64495	12.63263
14.65902	14.61245	14.57466	14.54356	14.51766	14.49584	14.47729
10.17815	10.17032	10.16393	10.15865	10.15423	10.15049	10.1473
12.76563	12.7502	12.73762	12.72722	12.71852	12.71118	12.70492
15.38245	15.35548	15.33352	15.31539	15.30024	15.28746	15.27657
18.03522	17.99181	17.9565	17.9274	17.90312	17.88266	17.86523
20.73099	20.66513	20.61168	20.56771	20.53107	20.50021	20.47398
12.46563	12.45605	12.44823	12.44175	12.43634	12.43176	12.42785
15.63464	15.61574	15.60033	15.5876	15.57695	15.56795	15.56028
18.83958	18.80655	18.77965	18.75744	18.73889	18.72324	18.7099
22.08855	22.03537	21.99214	21.95649	21.92676	21.90169	21.88035
25.39018	25.30951	25.24405	25.19019	25.14532	25.10753	25.0754
14.39407	14.38301	14.37397	14.3665	14.36024	14.35496	14.35044
18.05332	18.03151	18.01371	17.99901	17.98671	17.97632	17.96747
21.75407	21.71593	21.68487	21.65923	21.63781	21.61973	21.60434
25.50566	25.44425	25.39433	25.35318	25.31884	25.28989	25.26526
29.31805	29.2249	29.14932	29.08713	29.03531	28.99168	28.95458
16.09306	16.08069	16.07059	16.06223	16.05524	16.04933	16.04429
20.18423	20.15984	20.13995	20.1235	20.10975	20.09814	20.08824
24.32179	24.27915	24.24442	24.21575	24.19181	24.1716	24.15438
28.51619	28.44754	28.39172	28.34571	28.30733	28.27496	28.24742
32.77858	32.67443	32.58993	32.5204	32.46247	32.41368	32.3722
17.62907	17.61552	17.60445	17.5953	17.58763	17.58116	17.57563
22.11071	22.084	22.0622	22.04419	22.02913	22.01641	22.00556
26.64318	26.59648	26.55844	26.52703	26.5008	26.47866	26.4598
31.23792	31.16272	31.10158	31.05117	31.00912	30.97367	30.94349
35.90713	35.79305	35.70048	35.62431	35.56085	35.50741	35.46197
19.04157	19.02693	19.01498	19.00509	18.99682	18.98982	18.98385
23.8823	23.85344	23.8299	23.81045	23.79418	23.78044	23.76873
28.77793	28.72748	28.68639	28.65247	28.62413	28.60022	28.57985
33.74081	33.65959	33.59354	33.5391	33.49368	33.45539	33.42279
38.78413	38.66091	38.56093	38.47865	38.41011	38.35239	38.30331
20.35629	20.34065	20.32787	20.3173	20.30845	20.30097	20.29459
25.53125	25.5004	25.47524	25.45444	25.43705	25.42236	25.40984
30.7649	30.71097	30.66704	30.63078	30.60049	30.57492	30.55314
36.07045	35.98361	35.91301	35.85481	35.80625	35.76531	35.73047
41.46198	41.33025	41.22337	41.13541	41.06213	41.00042	40.94796
21.59111	21.57452	21.56096	21.54975	21.54036	21.53243	21.52567
27.07998	27.04726	27.02057	26.99851	26.98006	26.96448	26.9512
32.6311	32.5739	32.52731	32.48884	32.45672	32.4296	32.4065
38.25849	38.16638	38.0915	38.02976	37.97826	37.93484	37.89789
43.97707	43.83735	43.72398	43.63069	43.55297	43.48752	43.43187
22.75903	22.74154	22.72725	22.71543	22.70554	22.69718	22.69005
28.54481	28.51032	28.48218	28.45893	28.43949	28.42306	28.40906
34.3962	34.33591	34.28679	34.24625	34.21238	34.1838	34.15945
40.32798	40.2309	40.15196	40.08689	40.0326	39.98683	39.94788
46.35591	46.20862	46.08913	45.99079	45.90886	45.83987	45.78121

crack11.mcd This file will calculate the critical crack size for various Kic, s, and crack geometries.

$a := .00047625, .0009525 .. .0047625 \quad sy := 700, 750 .. 1000 \quad s := 200, 250 .. 400 \quad c(a) := a$

$$Q(a,c,s,sy) := \left[f(a,c)^2 - \left[.212 \cdot \left[\left(\frac{s}{sy} \right)^2 \right] \right] \right]$$

$$\Phi o \quad f(a,c) := \int_0^{\frac{\pi}{2}} \sqrt{\left[1 - \left(\frac{c^2 - a^2}{c^2} \right) \cdot \sin(\theta)^2 \right]} \, d\theta$$

$$K(a,c,s,sy) := 1.12 \cdot s \cdot \sqrt{\frac{\pi \cdot a}{Q(a,c,s,sy)}}$$

s
200
250
300
350
400

sy
700
750
800
850
900
950
$1 \cdot 10^3$

a	c(a)
$4.7625 \cdot 10^{-4}$	$4.7625 \cdot 10^{-4}$
$9.525 \cdot 10^{-4}$	$9.525 \cdot 10^{-4}$
0.00143	0.00143
0.00191	0.00191
0.00238	0.00238
0.00286	0.00286
0.00333	0.00333
0.00381	0.00381
0.00429	0.00429
0.00476	0.00476

Q(a,c(a),s,sy)
2.45009
2.45233
2.45415
2.45566
2.45693
2.458
2.45892
2.44036
2.44385
2.4467
2.44906
2.45104
2.45272
2.45415
2.42846
2.43348
2.43759
2.44099
2.44385
2.44626
2.44832
2.4144
2.42123
2.42682
2.43146
2.43534
2.43863
2.44143
2.39818
2.4071
2.4144
2.42045
2.42552
2.42982
2.43348
2.45009
2.45233
2.45415
2.45566
2.45693
2.458
2.45892
2.44036
2.44385
2.4467
2.44906
2.45104
2.45272
2.45415
2.42846

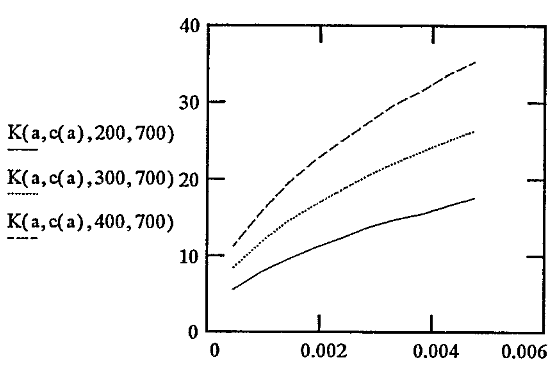

For this series of calculations, the crack is just twice as wide as it is deep (2c x a)(a/2c=.5)

K(a,c(a),s,700)	K(a,c(a),s,750)	K(a,c(a),s,800)	K(a,c(a),s,850)	K(a,c(a),s,900)	K(a,c(a),s,950)	K(a,c(a),s,1000)
5.5354	5.53288	5.53082	5.52912	5.52769	5.52649	5.52546
6.93304	6.92809	6.92405	6.92071	6.91791	6.91555	6.91353
8.34	8.33139	8.32437	8.31857	8.31371	8.30961	8.30611
9.75829	9.74452	9.73329	9.72401	9.71625	9.7097	9.70412
11.18999	11.16924	11.15233	11.13838	11.12673	11.1169	11.10853
7.82824	7.82468	7.82177	7.81936	7.81734	7.81563	7.81418
9.80479	9.7978	9.79209	9.78736	9.7834	9.78006	9.77721
11.79454	11.78237	11.77244	11.76423	11.75736	11.75156	11.74661
13.80031	13.78083	13.76494	13.75182	13.74085	13.73159	13.7237
15.82504	15.79569	15.77178	15.75205	15.73557	15.72167	15.70983
9.58759	9.58323	9.57967	9.57672	9.57424	9.57215	9.57037
12.00837	11.99981	11.99281	11.98702	11.98217	11.97808	11.97458
14.4453	14.4304	14.41824	14.40818	14.39977	14.39266	14.3866
16.90186	16.878	16.85854	16.84247	16.82904	16.8177	16.80803
19.38164	19.34568	19.31641	19.29224	19.27206	19.25504	19.24053
11.0708	11.06576	11.06165	11.05824	11.05539	11.05297	11.05091
13.86607	13.85618	13.8481	13.84142	13.83582	13.83109	13.82706
16.68	16.66279	16.64874	16.63713	16.62742	16.61921	16.61221
19.51658	19.48903	19.46657	19.44801	19.4325	19.41941	19.40824
22.37999	22.33847	22.30467	22.27676	22.25346	22.2338	22.21705
12.37753	12.3719	12.3673	12.36349	12.3603	12.3576	12.3553
15.50274	15.49168	15.48265	15.47518	15.46892	15.46363	15.45912
18.64881	18.62957	18.61386	18.60088	18.59002	18.58084	18.57302
21.8202	21.7894	21.76429	21.74354	21.7262	21.71156	21.69908
25.02159	24.97517	24.93738	24.90618	24.88013	24.85814	24.83942
13.5589	13.55274	13.5477	13.54352	13.54003	13.53707	13.53455
16.9824	16.97029	16.96039	16.95221	16.94535	16.93956	16.93462
20.42874	20.40767	20.39046	20.37624	20.36435	20.35429	20.34572
23.90283	23.86909	23.84158	23.81885	23.79986	23.78382	23.77015
27.40978	27.35893	27.31753	27.28335	27.25481	27.23073	27.21022
14.64529	14.63863	14.63318	14.62867	14.6249	14.62171	14.61898
18.34309	18.33001	18.31932	18.31047	18.30307	18.29682	18.29148
22.06556	22.0428	22.02422	22.00886	21.99601	21.98515	21.97589
25.81801	25.78157	25.75185	25.7273	25.70679	25.68946	25.67469
29.60594	29.55102	29.5063	29.46939	29.43856	29.41255	29.3904
15.65647	15.64935	15.64353	15.63871	15.63468	15.63126	15.62835
19.60959	19.5956	19.58417	19.57472	19.56681	19.56012	19.55441
23.58908	23.56474	23.54488	23.52846	23.51472	23.50311	23.49322
27.60062	27.56165	27.52989	27.50364	27.48171	27.46319	27.4474
31.65008	31.59137	31.54356	31.5041	31.47115	31.44334	31.41966
16.6062	16.59865	16.59247	16.58736	16.58308	16.57946	16.57637
20.79911	20.78427	20.77215	20.76213	20.75373	20.74664	20.74059
25.02	24.99418	24.97312	24.9557	24.94113	24.92882	24.91832
29.27487	29.23355	29.19986	29.17202	29.14875	29.12911	29.11237
33.56998	33.50771	33.457	33.41515	33.38019	33.3507	33.32558
17.50447	17.49651	17.49	17.48461	17.4801	17.47628	17.47303
21.92419	21.90855	21.89577	21.8852	21.87636	21.86888	21.8625
26.37339	26.34618	26.32398	26.30561	26.29026	26.27728	26.26622
30.85843	30.81487	30.77935	30.75001	30.72549	30.70478	30.68713
35.38587	35.32023	35.26677	35.22266	35.18581	35.15472	35.12825

crack12.mcd This file will calculate the critical crack size for various Kic, s, and crack geometries.

$a := .00047625, .0009525 .. .0047625 \quad sy := 700, 750 .. 1000 \quad s := 200, 250 .. 400$

$$c(a) := \frac{a}{2}$$

$$Q(a,c,s,sy) := \left[f(a,c)^2 - \left[.212\cdot\left[\left(\frac{s}{sy}\right)^2\right]\right]\right]$$

Φo $$f(a,c) := \int_0^{\frac{\pi}{2}} \sqrt{\left[1 - \left(\frac{c^2 - a^2}{c^2}\right)\cdot \sin(\theta)^2\right]}\, d\theta$$

$$K(a,c,s,sy) := 1.12\cdot s\cdot\sqrt{\frac{\pi\cdot a}{Q(a,c,s,sy)}}$$

s	sy	a	c(a)
200	700	$4.7625\cdot10^{-4}$	$2.38125\cdot10^{-4}$
250	750	$9.525\cdot10^{-4}$	$4.7625\cdot10^{-4}$
300	800	0.00143	$7.14375\cdot10^{-4}$
350	850	0.00191	$9.525\cdot10^{-4}$
400	900	0.00238	0.00119
	950	0.00286	0.00143
	$1\cdot10^3$	0.00333	0.00167
		0.00381	0.00191
		0.00429	0.00214
		0.00476	0.00238

Q(a,c(a),s,sy)
5.84932
5.85155
5.85338
5.85489
5.85616
5.85723
5.85815
5.83959
5.84307
5.84592
5.84829
5.85027
5.85195
5.85338
5.82769
5.83271
5.83681
5.84022
5.84307
5.84549
5.84755
5.81363
5.82046
5.82605
5.83068
5.83457
5.83785
5.84066
5.7974
5.80632
5.81363
5.81968
5.82475
5.82904
5.83271
5.84932
5.85155
5.85338
5.85489
5.85616
5.85723
5.85815
5.83959
5.84307
5.84592
5.84829
5.85027
5.85195
5.85338
5.82769

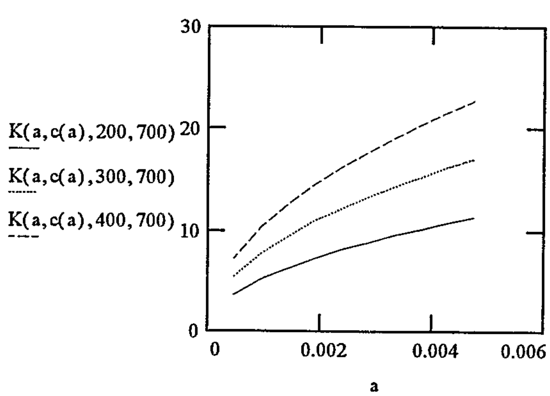

For this series of calculations, the crack is just as wide as it is deep (2c = a)(a/2c=1)

K(a,c(a),s,700)	K(a,c(a),s,750)	K(a,c(a),s,800)	K(a,c(a),s,850)	K(a,c(a),s,900)	K(a,c(a),s,950)	K(a,c(a),s,1000)
3.58251	3.58183	3.58127	3.58081	3.58042	3.58009	3.57981
4.48187	4.48053	4.47944	4.47854	4.47778	4.47714	4.47659
5.38373	5.38142	5.37952	5.37795	5.37664	5.37553	5.37458
6.28861	6.28492	6.28191	6.27941	6.27732	6.27555	6.27405
7.19704	7.19151	7.18699	7.18325	7.18012	7.17748	7.17522
5.06644	5.06547	5.06468	5.06403	5.06348	5.06302	5.06262
6.33832	6.33643	6.33489	6.33361	6.33253	6.33163	6.33085
7.61375	7.61047	7.60779	7.60558	7.60372	7.60215	7.60081
8.89344	8.88822	8.88396	8.88043	8.87747	8.87497	8.87284
10.17815	10.17032	10.16393	10.15865	10.15423	10.15049	10.1473
6.20509	6.20391	6.20294	6.20214	6.20147	6.2009	6.20042
7.76283	7.76051	7.75862	7.75705	7.75574	7.75463	7.75368
9.3249	9.32089	9.31761	9.31489	9.31262	9.31069	9.30905
10.8922	10.8858	10.88058	10.87626	10.87264	10.86958	10.86697
12.46563	12.45605	12.44823	12.44175	12.43634	12.43176	12.42785
7.16503	7.16366	7.16254	7.16162	7.16084	7.16019	7.15963
8.96374	8.96107	8.95888	8.95707	8.95556	8.95427	8.95318
10.76747	10.76283	10.75905	10.75591	10.75328	10.75106	10.74917
12.57723	12.56984	12.56381	12.55882	12.55464	12.55111	12.54809
14.39407	14.38301	14.37397	14.3665	14.36024	14.35496	14.35044
8.01074	8.00921	8.00797	8.00693	8.00606	8.00533	8.0047
10.02177	10.01878	10.01634	10.01431	10.01262	10.01118	10.00996
12.03839	12.03321	12.02898	12.02547	12.02254	12.02005	12.01794
14.06177	14.05351	14.04677	14.04119	14.03651	14.03256	14.02919
16.09306	16.08069	16.07059	16.06223	16.05524	16.04933	16.04429
8.77533	8.77366	8.77229	8.77115	8.7702	8.7694	8.76871
10.9783	10.97502	10.97235	10.97013	10.96827	10.9667	10.96536
13.1874	13.18173	13.17709	13.17325	13.17003	13.16731	13.16499
15.40389	15.39485	15.38746	15.38135	15.37623	15.3719	15.36821
17.62907	17.61552	17.60445	17.5953	17.58763	17.58116	17.57563
9.47844	9.47663	9.47515	9.47393	9.4729	9.47204	9.47129
11.85792	11.85438	11.85149	11.84909	11.84709	11.84539	11.84394
14.24402	14.23789	14.23288	14.22873	14.22526	14.22232	14.21981
16.63811	16.62834	16.62036	16.61376	16.60823	16.60355	16.59956
19.04157	19.02693	19.01498	19.00509	18.99682	18.98982	18.98385
10.13288	10.13094	10.12936	10.12806	10.12696	10.12603	10.12524
12.67665	12.67287	12.66977	12.66721	12.66507	12.66325	12.66171
15.2275	15.22095	15.21559	15.21115	15.20744	15.2043	15.20162
17.78689	17.77645	17.76791	17.76085	17.75494	17.74994	17.74568
20.35629	20.34065	20.32787	20.3173	20.30845	20.30097	20.29459
10.74754	10.74549	10.74381	10.74243	10.74126	10.74028	10.73944
13.44562	13.4416	13.43833	13.43561	13.43333	13.43141	13.42977
16.1512	16.14425	16.13857	16.13386	16.12993	16.12659	16.12375
18.86584	18.85477	18.84572	18.83823	18.83196	18.82666	18.82214
21.59111	21.57452	21.56096	21.54975	21.54036	21.53243	21.52567
11.3289	11.32674	11.32497	11.32351	11.32228	11.32125	11.32036
14.17292	14.1687	14.16524	14.16238	14.15998	14.15795	14.15622
17.02486	17.01753	17.01155	17.00659	17.00243	16.99892	16.99593
19.88634	19.87467	19.86513	19.85724	19.85063	19.84504	19.84027
22.75903	22.74154	22.72725	22.71543	22.70554	22.69718	22.69005

crack14.mcd This file will calculate the critical crack size for various Kic, s, and crack geometries.

$a := .00047625, .0009525 .. .0047625 \quad sy := 700, 750 .. 1000 \quad s := 200, 250 .. 400$

$c(a) := a \cdot 10$

$\Phi o \quad f(a,c) := \int_0^{\frac{\pi}{2}} \sqrt{\left[1 - \left(\frac{c^2 - a^2}{c^2}\right) \cdot \sin(\theta)^2\right]}\, d\theta$

$Q(a,c,s,sy) := \left[f(a,c)^2 - \left[.212 \cdot \left[\left(\frac{s}{sy}\right)^2\right]\right]\right]$

$K(a,c,s,sy) := 1.12 \cdot s \cdot \sqrt{\frac{\pi \cdot a}{Q(a,c,s,sy)}}$

s
200
250
300
350
400

sy
700
750
800
850
900
950
$1 \cdot 10^3$

a
$4.7625 \cdot 10^{-4}$
$9.525 \cdot 10^{-4}$
0.00143
0.00191
0.00238
0.00286
0.00333
0.00381
0.00429
0.00476

c(a)
0.00476
0.00953
0.01429
0.01905
0.02381
0.02858
0.03334
0.0381
0.04286
0.04763

f(a,c(a))
1.01599
1.01599
1.01599
1.01599
1.01599
1.01599
1.01599
1.01599
1.01599
1.01599

Q(a,c(a),s,sy)
1.01493
1.01716
1.01899
1.0205
1.02177
1.02284
1.02376
1.00519
1.00868
1.01153
1.0139
1.01588
1.01755
1.01899
0.9933
0.99832
1.00242
1.00583
1.00868
1.01109
1.01316
0.97924
0.98607
0.99166
0.99629
1.00017
1.00346
1.00627
0.96301
0.97193
0.97924
0.98529
0.99036
0.99465
0.99832
1.01493
1.01716
1.01899
1.0205
1.02177
1.02284
1.02376
1.00519
1.00868
1.01153
1.0139
1.01588
1.01755
1.01899
0.9933

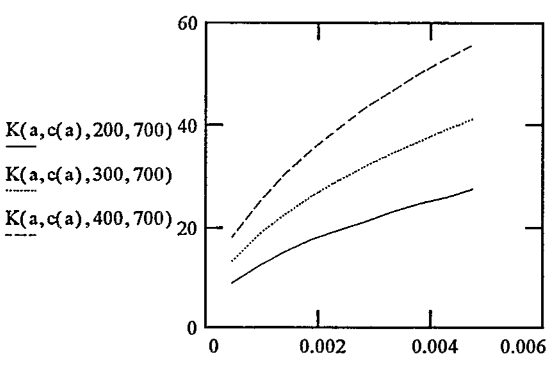

For this series of calculations, the crack is 20 times wider than it is deep (2c = 20a)(a/2c = .05)

K(a,c(a),s,700)	K(a,c(a),s,750)	K(a,c(a),s,800)	K(a,c(a),s,850)	K(a,c(a),s,900)	K(a,c(a),s,950)	K(a,c(a),s,1000)
8.60048	8.59104	8.58334	8.57698	8.57165	8.56716	8.56332
10.80253	10.78385	10.76863	10.75607	10.74558	10.73672	10.72918
13.04044	13.00762	12.98094	12.95895	12.94062	12.92516	12.912
15.32269	15.26952	15.22641	15.19097	15.16145	15.1366	15.11549
17.65854	17.5773	17.51164	17.45778	17.41302	17.37541	17.34349
12.16291	12.14957	12.13868	12.12968	12.12215	12.11579	12.11037
15.27708	15.25066	15.22914	15.21138	15.19654	15.18402	15.17335
18.44196	18.39555	18.35782	18.32673	18.3008	18.27893	18.26033
21.66955	21.59436	21.5334	21.48327	21.44153	21.40639	21.37653
24.97295	24.85806	24.7652	24.68902	24.62573	24.57254	24.5274
14.89646	14.88012	14.86678	14.85576	14.84654	14.83875	14.83211
18.71052	18.67817	18.65182	18.63006	18.61189	18.59655	18.58348
22.5867	22.52985	22.48365	22.44557	22.41381	22.38703	22.36424
26.53967	26.44758	26.37292	26.31152	26.2604	26.21737	26.18079
30.58549	30.44478	30.33105	30.23776	30.16023	30.09509	30.03981
17.20095	17.18208	17.16668	17.15395	17.14331	17.13431	17.12664
21.60505	21.56769	21.53726	21.51214	21.49115	21.47344	21.45835
26.08087	26.01523	25.96188	25.91791	25.88123	25.85032	25.82401
30.64537	30.53904	30.45283	30.38193	30.3229	30.27321	30.23097
35.31708	35.1546	35.02328	34.91555	34.82604	34.75082	34.68698
19.23125	19.21015	19.19294	19.1787	19.1668	19.15674	19.14817
24.15518	24.11342	24.07939	24.0513	24.02784	24.00804	23.99117
29.1593	29.08592	29.02626	28.9771	28.9361	28.90153	28.87212
34.26257	34.14368	34.0473	33.96803	33.90203	33.84648	33.79926
39.48569	39.30404	39.15722	39.03678	38.93669	38.8526	38.78122
21.06678	21.04367	21.02481	21.00922	20.99618	20.98516	20.97577
26.46068	26.41492	26.37765	26.34688	26.32118	26.29949	26.28101
31.94242	31.86203	31.79668	31.74283	31.69791	31.66004	31.62782
37.53276	37.40253	37.29694	37.21011	37.13781	37.07696	37.02523
43.25441	43.05542	42.89458	42.76264	42.65301	42.56089	42.4827
22.75472	22.72976	22.70939	22.69255	22.67846	22.66656	22.65642
28.5808	28.53138	28.49112	28.45789	28.43012	28.40669	28.38673
34.50175	34.41492	34.34434	34.28617	34.23765	34.19675	34.16195
40.54001	40.39935	40.2853	40.19152	40.11342	40.04769	39.99182
46.7201	46.50516	46.33144	46.18894	46.07052	45.97101	45.88656
24.32582	24.29913	24.27736	24.25935	24.2443	24.23158	24.22073
30.55416	30.50133	30.45829	30.42276	30.39308	30.36803	30.3467
36.88393	36.7911	36.71564	36.65346	36.60159	36.55787	36.52066
43.3391	43.18872	43.0668	42.96654	42.88305	42.81278	42.75305
49.94589	49.71611	49.5304	49.37805	49.25146	49.14508	49.0548
25.80143	25.77312	25.75002	25.73093	25.71496	25.70147	25.68997
32.40758	32.35154	32.30589	32.26821	32.23673	32.21016	32.18753
39.12131	39.02285	38.94282	38.87686	38.82185	38.77547	38.73601
45.96806	45.80855	45.67924	45.5729	45.48435	45.40981	45.34646
52.97562	52.7319	52.53492	52.37333	52.23906	52.12623	52.03047
27.19709	27.16726	27.14291	27.12278	27.10595	27.09173	27.0796
34.16059	34.10152	34.0534	34.01368	33.9805	33.95249	33.92864
41.23748	41.1337	41.04934	40.97981	40.92182	40.87294	40.83134
48.45458	48.28645	48.15015	48.03805	47.94471	47.86614	47.79937
55.8412	55.5843	55.37667	55.20634	55.0648	54.94587	54.84493

crack15.mcd This file will calculate the critical crack size for various Kic, s, and crack geometries.

$i := 0.1, .2 .. .6 \qquad ssy := 0.2, 0.4 .. 1.0 \quad a := 1$

$c(i) := \dfrac{a}{i \cdot 2}$

Φo

$$f(a,c) := \int_0^{\frac{\pi}{2}} \sqrt{\left[1 - \left(\frac{c^2 - a^2}{c^2}\right) \cdot \sin(\theta)^2\right]}\, d\theta$$

$$Q(a,c,ssy) := \left[f(a,c)^2 - \left[.212 \cdot \left[(ssy)^2\right]\right]\right]$$

$a = 1$

$Q(a,c(i),ssy)$
1.09508
1.06964
1.02724
0.96788
0.89156
1.31553
1.29009
1.24769
1.18833
1.11201
1.62059
1.59515
1.55275
1.49339
1.41707
2.00248
1.97704
1.93464
1.87528
1.79896
2.45892
2.43348
2.39108
2.33172
2.2554
2.98943
2.96399
2.92159
2.86223
2.78591

$f(a,c(i))$	$c(i)$
1.0505	5
1.15066	2.5
1.27635	1.66667
1.41808	1.25
1.5708	1
1.73145	0.83333

ssy
0.2
0.4
0.6
0.8
1

$\dfrac{a}{2 \cdot c(i)}$
0.1
0.2
0.3
0.4
0.5
0.6

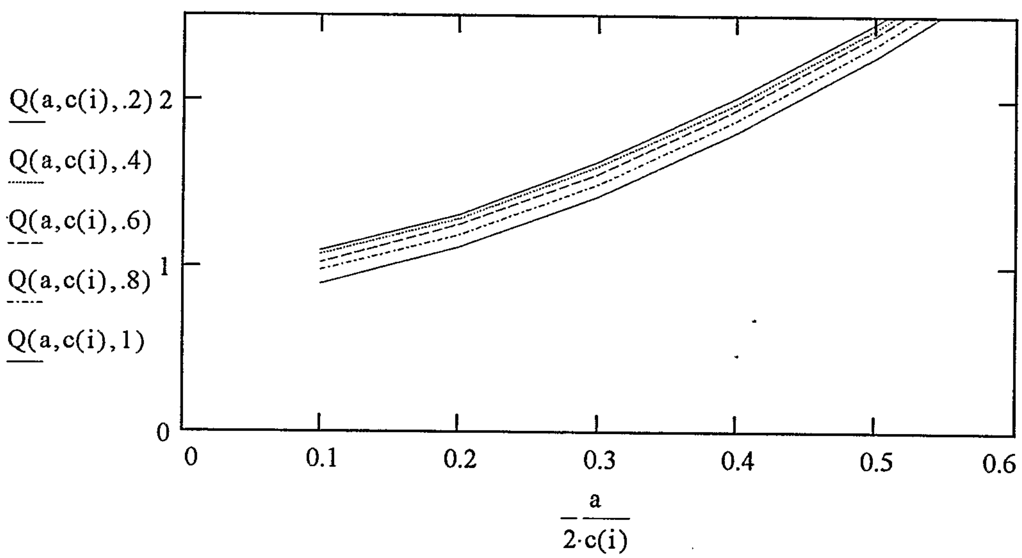

dipcrk6.mcd

This file will calculate the elliptic integral to find the "free surface correction factor" for the stress intensity factor equation for a surface crack.

$a := .00047625, .0009525 .. .0047625$

$c(a) := 100 \cdot a$

$\Phi o \qquad f(a,c) := \int_0^{\frac{\pi}{2}} \sqrt{\left[1 - \left(\frac{c^2 - a^2}{c^2}\right) \cdot (\sin(\theta))^2\right]} \, d\theta$

f(a, 10·a)	f(a, a)	f(a, a/10)
1.01599	1.570796	10.1599
1.01599	1.570796	10.1599
1.01599	1.570796	10.1599
1.01599	1.570796	10.1599
1.01599	1.570796	10.1599
1.01599	1.570796	10.1599
1.01599	1.570796	10.1599
1.01599	1.570796	10.1599
1.01599	1.570796	10.1599
1.01599	1.570796	10.1599

....

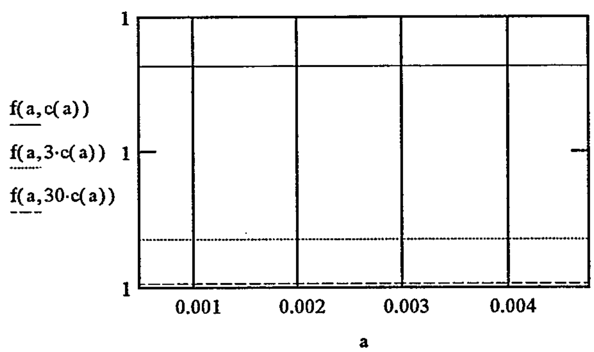

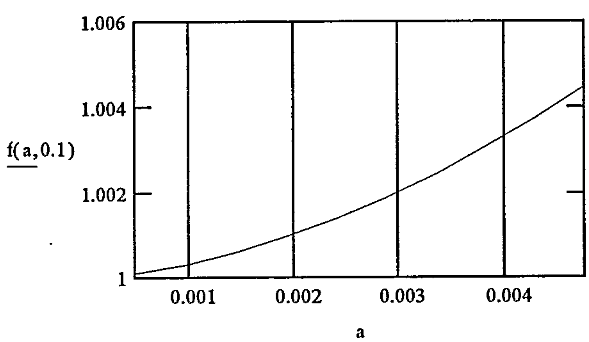

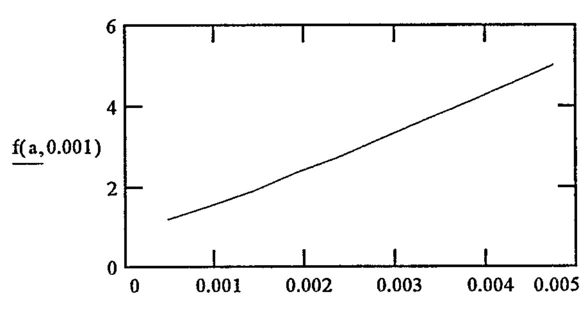

crack6.mcd

This file calculates critical crack size for a through-thickness crack 2a wide in the center of a plate under tension.

$s := 200, 250 .. 900$ (MPa) stress in material

$K := 40, 50 .. 220$ MPa root m

$$a(K,s) := \frac{K^2}{s^2 \cdot \pi} \cdot 39.37$$

Critical crack size (in)

K	s	$2 \cdot a(40,s)$	$a(50,s) \cdot 2$	$a(60,s) \cdot 2$	$a(70,s) \cdot 2$
40	200	1.003	1.566	2.256	3.07
50	250	0.642	1.003	1.444	1.965
60	300	0.446	0.696	1.003	1.365
70	350	0.327	0.512	0.737	1.003
80	400	0.251	0.392	0.564	0.768
90	450	0.198	0.309	0.446	0.606
100	500	0.16	0.251	0.361	0.491
110	550	0.133	0.207	0.298	0.406
120	600	0.111	0.174	0.251	0.341
130	650	0.095	0.148	0.214	0.291
140	700	0.082	0.128	0.184	0.251
150	750	0.071	0.111	0.16	0.218
160	800	0.063	0.098	0.141	0.192
170	850	0.056	0.087	0.125	0.17
180	900	0.05	0.077	0.111	0.152
190					
200					
210					
220					

$a(80,s) \cdot 2$	$a(90,s) \cdot 2$	$a(100,s) \cdot 2$	$a(110,s) \cdot 2$	$a(120,s) \cdot 2$	$a(130,s) \cdot 2$	$a(140,s) \cdot 2$
4.01	5.075	6.266	7.582	9.023	10.589	12.281
2.567	3.248	4.01	4.852	5.775	6.777	7.86
1.782	2.256	2.785	3.37	4.01	4.706	5.458
1.309	1.657	2.046	2.476	2.946	3.458	4.01
1.003	1.269	1.566	1.895	2.256	2.647	3.07
0.792	1.003	1.238	1.498	1.782	2.092	2.426
0.642	0.812	1.003	1.213	1.444	1.694	1.965
0.53	0.671	0.829	1.003	1.193	1.4	1.624
0.446	0.564	0.696	0.842	1.003	1.177	1.365
0.38	0.481	0.593	0.718	0.854	1.003	1.163
0.327	0.414	0.512	0.619	0.737	0.864	1.003
0.285	0.361	0.446	0.539	0.642	0.753	0.873
0.251	0.317	0.392	0.474	0.564	0.662	0.768
0.222	0.281	0.347	0.42	0.5	0.586	0.68
0.198	0.251	0.309	0.374	0.446	0.523	0.606

a(150,s)	a(160,s)	a(170,s)	a(180,s)	a(190,s)	a(200,s)	a(210,s)	a(220,s)
7.049	8.02	9.054	10.151	11.31	12.532	13.816	15.164
4.511	5.133	5.795	6.497	7.238	8.02	8.842	9.705
3.133	3.565	4.024	4.511	5.027	5.57	6.141	6.739
2.302	2.619	2.956	3.315	3.693	4.092	4.511	4.951
1.762	2.005	2.264	2.538	2.828	3.133	3.454	3.791
1.392	1.584	1.788	2.005	2.234	2.475	2.729	2.995
1.128	1.283	1.449	1.624	1.81	2.005	2.211	2.426
0.932	1.061	1.197	1.342	1.496	1.657	1.827	2.005
0.783	0.891	1.006	1.128	1.257	1.392	1.535	1.685
0.667	0.759	0.857	0.961	1.071	1.186	1.308	1.436
0.575	0.655	0.739	0.829	0.923	1.023	1.128	1.238
0.501	0.57	0.644	0.722	0.804	0.891	0.982	1.078
0.441	0.501	0.566	0.634	0.707	0.783	0.864	0.948
0.39	0.444	0.501	0.562	0.626	0.694	0.765	0.84
0.348	0.396	0.447	0.501	0.559	0.619	0.682	0.749

APPENDIX D

Calculations for Minimum CVN Impact Energy

crack16.mcd

This file calculates absorbed impact energy for several compositions based upon reference 2. To meet the ASME minimum for lateral expansion of 0.015 in., CVN (J) must be at least 32.

$FN := 0, 1 .. 15$ $\qquad\qquad$ $Ni := 8.0, 8.5 .. 15.0$

$CVN(FN, C, Ni) := 19 - 1.4 \cdot FN - 890 \cdot C^2 + 1.4 \cdot Ni$

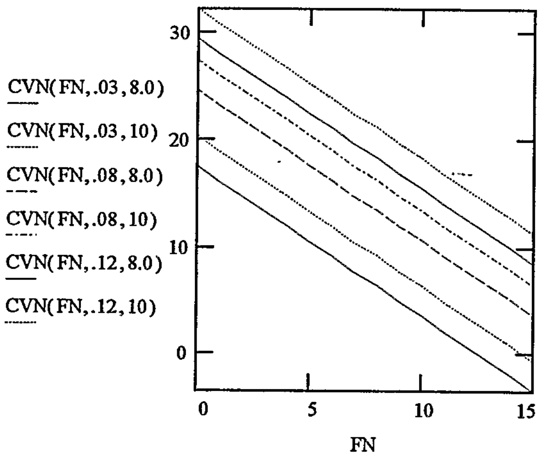

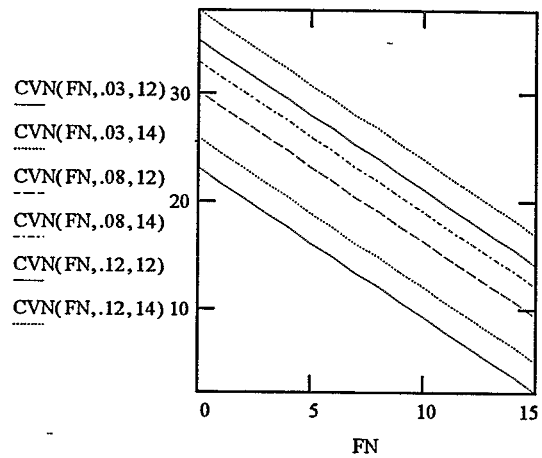

$C := .02, .03 .. .2$